

1 **Stability of ENSO and its tropical Pacific teleconnections**

2 **over the Last Millennium**

3 Sophie C. Lewis^{1*} and Allegra N. LeGrande²

4 [1] Research School of Earth Sciences, The Australian National University, Canberra, ACT, Australia
5 and ARC Centre of Excellence for Climate System Science

6 [2] NASA Goddard Institute for Space Studies and Center for Climate Systems Research, Columbia
7 University, 2880 Broadway, New York, NY, 10025, USA

8 [*] Corresponding author: Tel: +61 2 6215 0920, email: sophie.lewis@anu.edu.au

9

10 **Abstract**

11 Determining past changes in the amplitude, frequency and teleconnections of the El Niño-Southern
12 Oscillation (ENSO) is important for understanding its potential sensitivity to future anthropogenic
13 climate change. Palaeo-reconstructions from proxy records can provide long-term information of
14 ENSO interactions with the background climatic state through time. However, it remains unclear how
15 ENSO characteristics have changed on long timescales, and precisely which signals proxies record.
16 Proxy interpretations are typically underpinned by the assumption of stationarity in relationships
17 between local and remote climates, and often utilise archives from single locations located in the
18 Pacific Ocean to reconstruct ENSO histories. Here, we investigate the long-term characteristics of
19 ENSO and its teleconnections using the Last Millennium experiment of CMIP5 (Coupled Model
20 Intercomparison Project phase 5) (Taylor et al., 2012). We show that the relationship between ENSO
21 conditions (NINO3.4) and local climates across the Pacific basin differs significantly for 100-year
22 epochs defining the Last Millennium and the historical period of 1906-2005. Furthermore, models
23 demonstrate decadal- to centennial- scale modulation of ENSO behaviour during the Last
24 Millennium.. Overall, results suggest that the stability of teleconnections may be regionally dependent
25 and that proxy climate records may reveal complex changes in teleconnected patterns, rather than
26 large-scale changes in base ENSO characteristics. As such, proxy insights into ENSO may require
27 evidence to be considered over large spatial areas in order to deconvolve changes occurring in the
28 NINO3.4 region from those relating to local climatic variables. To obtain robust histories of the
29 ENSO and its remote impacts, we recommend interpretations of proxy records should be considered
30 in conjunction with palaeo-reconstructions from within the central Pacific.

33 **1. Introduction**

34 The El Niño-Southern Oscillation (ENSO) is an important determinant of climate variability, altering
35 global rainfall patterns and modulating global temperatures. Understanding the long-term
36 characteristics of ENSO variability and its sensitivity to external forcings, such as greenhouse gases,
37 represents a fundamental climate modelling and data challenge. While changes in ENSO behaviour
38 may occur under future global warming (Power et al., 2013), previous studies indicate a large
39 dispersion in global climate model (GCM) projections of changes in ENSO characteristics (e.g.
40 Collins et al., 2010; Vecchi and Wittenberg, 2010), and hence the sensitivity of the coupled ocean-
41 atmosphere system to future changing boundary conditions may be uncertain (DiNezio et al., 2012).
42 Recent model-based studies suggest changes toward more extreme ENSO occur under future
43 greenhouse warming (Power et al., 2013; Cai et al., 2014). However, investigations of the sensitivity
44 of ENSO to anthropogenic climate change are restricted by the relatively short instrumental record,
45 which provides us with limited guidance for understanding the range of ENSO behaviours. For
46 example, the observed changes in the character of ENSO in the 20th and 21st centuries (including
47 dominance of El Niño, rather than La Niña, episodes from the mid-1970s, and a La Niña-like mean
48 state since the 1990s (England et al., 2014)) are difficult to evaluate in terms of a forced response or
49 unforced variability given the limited observational record almost certainly does not capture the full
50 range of internal climate dynamics.

51 High resolution palaeo-reconstructions, including from tree rings, sediment cores, corals and
52 speleothems, have the potential to provide long-term information about changes in modes of climatic
53 variability and their sensitivity to different boundary conditions. Some tropical proxy records reveal
54 ENSO interactions with the background mean climatic state. For example, data from long-lived fossil
55 corals are often interpreted quantitatively as estimates of ENSO changes through time that show a
56 range of ENSO frequencies and amplitudes through time. Central Pacific coral reconstructions
57 generally reveal a weakened ENSO during the early Holocene (McGregor et al., 2013) and highly
58 variable ENSO activity throughout the Holocene (Cobb et al., 2013), which may have arisen from
59 internal ocean-atmosphere variability (Cobb et al., 2003). Developing robust estimates of natural
60 ENSO variability over a period longer than permitted through the instrumental record is a useful
61 research avenue, with the potential for informing meaningful adaptive strategies for future climate
62 change.

63 Palaeo-ENSO proxy records of the Last Millennium (1,000 years) are sparsely populated temporally
64 and spatially, and reconstructions remain uncertain (Cobb et al., 2003; Khider et al., 2011). It also
65 remains unclear as to precisely which climatic signals associated with ENSO are being recorded in
66 these individual proxy records and whether these provide the necessary resolution to reconstruct
67 ENSO changes. The assumption of stationarity of relationships between local and remote climates

68 (teleconnections) underpins the interpretation of many palaeoclimate reconstructions, although
69 stationarity should not necessarily be assumed in terms of ENSO variability (Gallant et al., 2013). Are
70 palaeo-reconstructions from the tropical Pacific recording base changes in the ENSO system or rather
71 changes in teleconnected patterns? Previous model-based studies have identified sensitivity in the
72 relationship between ENSO and the background climate state, and urged caution in the reconstruction
73 of ENSO from proxy records under the assumption of stationarity of observed teleconnections (Coats
74 et al., 2013; Gallant et al., 2013).

75 However, these studies have not comprehensively addressed the degree to which uncertainty about the
76 non-stationarity of ENSO teleconnections can be assessed for particular locations and for particular
77 mean climatic states. Furthermore, although we previously investigated the potential non-stationarity
78 of hydrologic responses to ENSO-like conditions under disparate boundary conditions in idealised
79 model simulations, we did not provide guidance for interpreting tropical proxy records in particular
80 regions (Lewis et al., 2014), which currently comprise our dominant source of information about
81 ENSO characteristics beyond the instrumental record. In addition, while previous studies have utilised
82 proxy records, together with simulations using global climate models (GCMs) to evaluate the
83 representation of ENSO in the current generation of GCMs (Cobb et al., 2013), these approaches
84 focused on using palaeo-ENSO reconstructions to test the performance of GCMs for the purpose of
85 constraining uncertainty in future projections of ENSO behaviour under climate change.

86 As such, precisely which expressions of ENSO are being recorded in proxy archives under differing
87 climatic boundary conditions have not been comprehensively interrogated. Climate models, in
88 addition to observational and proxy climate evidence, allow an understanding of long-term ENSO
89 changes through time to be obtained (Schmidt, 2010). A new generation of climate models and
90 experiments has recently become available (Taylor et al., 2012), providing an opportunity for the first
91 time to investigate ~1200 years of ENSO variability and establish a framework for understanding
92 ENSO changes through time, using more models than previously possible. Hence in this current
93 study, we investigate changes in ENSO characteristics (frequency and amplitude) in model
94 experiments of the Last Millennium ('past1000'). Focusing on three key climatic regions (East,
95 Central and West Pacific), where explicit palaeo-ENSO reconstructions have been made,
96 teleconnected patterns (the relationship between local and remote climates) throughout the Last
97 Millennium are examined for surface temperatures and precipitation. We ultimately aim to determine
98 whether proxy archives in the tropical Pacific are likely to be recording alterations in ENSO base
99 frequencies or local-scale teleconnections under differing boundary conditions.

100 **2. Datasets and methods**

101 **2.1 Definitions**

102 The study is primarily focused on palaeo-ENSO variability from the tropical Pacific. Model data were
103 investigated in three regions that have been identified as sensitive to modern ENSO variability and
104 have also been used explicitly to reconstruct past ENSO changes (e.g. Cobb et al., 2013; McGregor et
105 al., 2013). Area-mean anomalies for precipitation and surface temperature were calculated for the
106 West (10°S-10°N, 105°-155°E), Central (10°S-10°N, 170°-130°W) and East Pacific (20°S-5°N, 65°-
107 90°W) region and surface temperature for the NINO3.4 region (5°N - 5°S, 170° - 120°W) (Fig. 1).
108 These regions are not intended to provide exhaustive coverage of ENSO impacts, but are large enough
109 to provide useful comparisons with model-based data.

110 El Niño episodes were defined based on simulated surface air temperature anomalies in the NINO3.4
111 region, with events defined in the models when NINO3.4 temperature anomalies were >0.5 K for at
112 least six consecutive months (Trenberth, 1997). Conversely, La Niña episodes were defined when
113 NINO3.4 temperature anomalies were <-0.5 K for at least six consecutive months. Spatial patterns are
114 examined by compositing monthly temperature and rainfall anomalies into positive (El Niño) and
115 negative (La Niña) phases using these definitions for all CMIP5 models analysed (Figs 1 and 2). We
116 utilise the NINO3.4 region as an index to classify ENSO conditions. Although the NINO3.4 region is
117 commonly used to categorise ENSO episodes, it should be noted that there are other indices of ENSO
118 that may also provide useful information beyond the central tropical Pacific conditions described by
119 the NINO3.4 (see Supplementary Figs 1-3).

120 **2.2 Model experiments**

121 CMIP5 data (Taylor et al., 2012) were downloaded from the Project for Model Diagnosis and
122 Intercomparison (PCMDI) through the Australian Earth System Grid (ESG) node. Simulations were
123 used of the historical (1850-2005 CE) experiment, which is forced using changing atmospheric
124 compositions due to observed anthropogenic and volcanic influences, solar forcings and emissions of
125 short-lived species from natural and anthropogenic aerosols. In addition, simulations were used of the
126 Last Millennium (past1000) (850-1849 CE), in which reconstructed time evolving exogenous forcings
127 are imposed, including changes in volcanic aerosols, well-mixed greenhouse gases, land use, orbital
128 parameters and solar changes. Each model's pre-industrial control simulation (piControl) with non-
129 evolving pre-industrial forcings was analysed.

130 Data (precipitation (pr) and surface temperature (ts)) for six remaining models were regridded onto a
131 common 1.5° latitude by 1.5° longitude grid. For the piControl and past1000 experiments, monthly
132 anomalies were calculated by subtracting the mean seasonal cycle for each model. For the historical
133 experiment the 100-year period of 1906-2005 is considered. Additional experiments were analysed
134 for CMIP5-participating models, where available. For GISS-E2-R and IPSL-CM5A-LR models,
135 extended control simulations of >500 years in duration were analysed and compared to forced,
136 past1000 experiments.

137 **2.3. Models and evaluation**

138 The basic properties of El Niño-Southern Oscillation (ENSO) simulated in Coupled Model
139 Intercomparison Project phase 5 (CMIP5) models (Taylor et al., 2012), relative to observations, have
140 been comprehensively evaluated in previous studies (e.g., Bellenger et al., 2013; Guilyardi et al.,
141 2012). For example, Bellenger et al (2013) examined ENSO through 6 metrics - 1) ENSO amplitude
142 (Niño3 sea surface temperature (SST) standard deviation), 2) structure (Niño3 vs. Niño4 amplitude),
143 3) frequency (root mean square error of Niño3 SST anomaly spectra), 4) heating source (Niño4
144 precipitation standard deviation), 5) the amplitude of the ENSO biennial component (the ratio of the
145 Niño3 SST anomaly timeseries power in the 3–8 years and 1–3 years bands) and 6) seasonality of
146 ENSO (ratio between winter November-January over spring March– May average Niño3 SST
147 anomalies standard deviations. This study showed a significant improvement in model skill compared
148 with CMIP3 generation models, including improved sea surface temperature anomaly location,
149 seasonal phase locking and ENSO amplitude.

150 In our current study, all CMIP5 models were analysed where past1000 simulations were archived on
151 the Australian ESG node. This provided nine models for selection, although bcc-csm1-1 was excluded
152 from analysis because its dominant ENSO periodicity is too short and MIROC-ESM model was also
153 excluded, as it exhibits large drift related error in the form of long-term trends that cannot be
154 attributed to natural variability (Gupta et al., 2013) (see Supplementary Fig. 4). We use the remaining
155 seven models with CMIP5 Last Millennium simulations (see Table 1). For GISS-E-2-R, we include
156 only one contributing realisation (r1i1p121) to constitute a multi-model ensemble of one member
157 from each model.

158 Models were compared to twentieth century reanalysis data (20CR) (Compo and Whitaker, 2011),
159 which is widely used a proxy of observed climate (King et al., 2014; Klingaman and Woolnough,
160 2013). In order to focus on ENSO characteristics, we compare these datasets for the period of 1976-
161 2005, rather than an extended historical period, due to greenhouse forced non-stationarities over the
162 post-industrial era. It should be noted that ENSO properties have changed over the last several
163 decades, in particular with increased frequency of Central Pacific-centred events in recent decades,
164 which have substantially different characteristics (Pascolini-Campbell et al., 2014). Hence model skill
165 in recent decades does not ensure that all ‘flavours’ of ENSO are equally well captured. CMIP5
166 historical simulations were compared to reanalysis precipitation and surface temperature over the
167 1976-2005 period for several ENSO-related characteristics.

168 To investigate the model representation of ENSO spatial patterns, the first empirical orthogonal
169 function of the tropical Pacific surface temperature anomalies was calculated for 20CR reanalysis and
170 CMIP5 multi-model mean (MMM) EOF (Figs 3a and 3b). Precipitation anomalies were also analysed
171 (Figs 3c and 3d). Surface temperature and precipitation patterns are qualitatively similar for reanalysis

172 and models; temperature patterns are generally of the same sign, although the meridional width of
173 tropical temperature anomalies is narrower than in the reanalysis estimates, and simulated
174 precipitation patterns are similar to the reanalysis estimate in the central Pacific, although positive
175 anomalies are located too far westward in the CMIP5 MMM, compared with observations. In
176 addition, the relationship between NINO3.4 surface temperature anomalies and global precipitation
177 fields in reanalysis was compared to the CMIP5 MMM (Figs 3e and 3f). The correlation coefficients
178 between NINO3.4 temperature anomalies and local precipitation are generally of the same sign in
179 simulated and reanalysis fields, including positive correlations in the Central and East Pacific and
180 negative correlations in the west Pacific. These reanalysis-model comparisons are broadly insightful
181 about the model representations of ENSO.

182 **3 Diagnosing ENSO changes and teleconnections**

183 The location of ENSO activity in the historical and Last Millennium experiments was first explored
184 using the leading empirical orthogonal function (EOF) of the tropical Pacific surface temperature.
185 These spatial patterns were compared to the NINO3.4 index to determine possible non-stationarities
186 in the site of ENSO activity through time (Li et al., 2011). This EOF analysis (Supplementary Fig. 5)
187 demonstrates that in both experiments, the surface temperature patterns are loaded in the NINO3.4
188 region. Although there are some differences in the spatial patterns of the leading EOF mode across the
189 equatorial Pacific, the similarity in model experiments in this particular region indicates that areal-
190 average NINO3.4 temperatures provide a useful metric of ENSO activity in both experiments. An
191 EOF analysis does not necessarily reveal modes that can be readily interpreted physically. However,
192 in this study utilise an identical set of models for each experiment, and hence possible biases in ENSO
193 representations in the models are not considered prohibitive to investigating changes in the stability of
194 teleconnections through time.

195 A wavelet analysis was next used to examine the frequency and amplitude of NINO3.4 surface
196 temperature variability in each model for statistically significant changes. Wavelet analysis is useful
197 for examining non-stationary signal and provides time and frequency localisation. A Morlet mother
198 wavelet (Torrence and Compo, 1998) with degree 6 was used to calculate the wavelet power spectra
199 and identify large-scale changes in variance. Wavelet spectral estimates were tested against red noise,
200 represented as a first order autoregressive process. The NINO3.4 mean wavelet power spectrum,
201 generated using a Morlet wavelet of degree 6, was used as a metric for ENSO amplitude. The spectral
202 power was calculated for the historical simulation (years 1906-2005) and compared to the range of
203 spectral power displayed in the past1000 experiment, calculated using ten 100-year epochs (Fig. 4).

204 The relationship between ENSO variability and teleconnected patterns in the tropical Pacific regions
205 (East, Central and West) was diagnosed through several complementary approaches. First, an
206 ordinary least squares regression between monthly NINO3.4 mean surface temperature and remote

207 area-mean surface temperature, and between monthly NINO3.4 mean surface temperature and remote
208 area-mean precipitation was compared for the historical and Last Millennium experiments, for each
209 region. Second, the relationship between local and NINO3.4 climates was considered using the
210 correlation between variables ($\text{Corr}(\text{Local}, \text{Remote})$), analogous to considering land-surface coupling
211 strength (Lorenz et al., 2012). Correlations coefficients were calculated for monthly timeseries in ten
212 100-year epochs comprising the Last Millennium. Values were determined at each model gridbox and
213 an area-weighted mean calculated for each region. The significance of correlations was assessed at the
214 95% confidence level for each coefficient using a t-test. Third, the significance of identified changes
215 in local-remote relationships during the Last Millennium was investigated.

216 For each 100-year epoch comprising the Last Millennium, the El Niño- and La Niña- associated local
217 temperature and precipitation anomalies were selected for each region. A two-sided Kolmogorov-
218 Smirnov (KS-) test was used to investigate whether the distribution of local climate variables in 100-
219 year epochs within the Last Millennium could statistically have been drawn from the same population
220 (at the 5% significance level). A two-sided KS-test was applied to each ENSO phase for each variable
221 (surface temperature, precipitation) in each region (East, Central, West) comparing every permutation
222 of epochs sequentially (e.g. comparing El Niño-associated Central Pacific temperatures during 850-
223 949 with 950-1049, then 1050-1149, then 1150-1249 etc.). A KS-test was used for detecting changes
224 in ENSO-remote climate relationships in Last Millennium timeseries as it is non-parametric and
225 requires no assumptions to be made regarding the distribution of the data. A change is detected where
226 the null hypothesis (that the distributions considered were drawn from the same population) is
227 rejected at the 5% significance level.

228 **4. ENSO during the Last Millennium**

229 **4.1 ENSO characteristics**

230 Models demonstrate a range of variance in the ENSO-relevant band (2-8 years) for the historical
231 experiment (Fig. 4). In the historical experiment, ENSO amplitude is generally weaker at relevant
232 periods for the MRI-CGMC3, GISS-E2-R and HadCM3 models. Notably, the amplitude of higher
233 ENSO-relevant periods (6-8 years) in the historical simulations is generally outside the range
234 exhibited in the Last Millennium for each model (Fig. 2). However, previous model-based studies
235 (Coats et al., 2013; Wittenberg, 2009) that reveal strong inter-decadal to inter-centennial modulation
236 of ENSO behaviour warn that such modulation may not be fully revealed by the comparatively short
237 instrumental climate record available. Hence, large uncertainties may exist in ENSO metrics
238 diagnosed from short records.

239

240 Decadal- to centennial-scale El Niño- and La Niña-like episodes during the Last Millennium
241 simulations are evident in all models analysed here (Fig. 5). This low frequency modulation may

242 result from internal variability (e.g., Karnauskas et al., 2012; Borlace et al., 2013), or may be relate to
243 external forcings. For example, external forcings from large tropical volcanic eruptions occurring
244 between 1250 and 1600 CE (Supplementary Fig. 6), may produce decadal- to centennial-scale ENSO
245 responses, which are discussed further in section 6. Alternatively, decadal- to centennial-scale
246 modulation of ENSO behaviour may result from internal ocean-atmosphere dynamics rather than a
247 response to exogenous forcings. The properties of ENSO simulated in the control simulations (Fig. 6)
248 that do not impose external forcings, exhibit qualitatively similar variability to that shown in the
249 externally forced Last Millennium experiment (Fig. 5). This similarity includes multi-decadal to
250 centennial- scale El Niño- and La Niña-like phases.

251

252 **4.2 ENSO impacts and teleconnections**

253 Models show broadly similar global impacts associated with NINO3.4 regional temperature
254 anomalies in the Last Millennium and historical experiments (Figs. 1 and 2). The composited patterns
255 of global surface air temperature anomalies associated with positive (El Niño) and negative (La Niña)
256 ENSO phases derived from all analysed models spatially coherent across the experiments. However,
257 both El Niño and La Niña anomalies associated with the historical period (1906-2005) are generally
258 of greater magnitude than for the Last Millennium, for the MMM and in various models including
259 FGOALS-s2 and CCSM4. These experiments are most similar in the tropical Pacific, with larger
260 differences evident at remote locations outside the equatorial Pacific, including over North America
261 and the south Pacific.

262 The relationship between NINO3.4 regional temperature anomalies and the mean local climate is
263 examined in each analysed Pacific region (East, Central, West) using the correlation between
264 variables ($\text{Corr}(\text{Local}, \text{Remote})$). This approach is analogous to considering land-surface coupling
265 strength (Lorenz et al. 2012). We diagnose temporal stability using this correlation in ten 100-year
266 epochs that comprise the Last Millennium and the 100-year historical period of 1906-2005 (Figs 7
267 and 8). The strength of the remote-local relationship varies temporally and is also both regionally and
268 climate variable dependent. In the West Pacific, particularly, this coupling is generally weak and not
269 found to be statistically significant for most epochs and models. It is notable that the strongest West
270 Pacific-NINO3.4 correlation for the MMM, and FGOALS-s2 and IPSL-CM5A-LR models is
271 calculated for the historical experiment. There is, however, a large dispersion in correlations
272 calculated across the models, with negative correlations calculated from CCSM4, which also shows
273 the strongest El Niño-related cool features in the Warm Pool region (Figs 1 and 2). The remote- local
274 temperature relationship is consistently stronger in the East and Central Pacific regions. The strongest
275 local precipitation coupling occurs for the Central Pacific, with no statistically significant
276 relationships found for the West and East Pacific across the model ensemble (with the exception of
277 CCSM4) (Fig. 8).

278 We also investigate the significance of identified Last Millennium changes in local-remote
279 relationship across these epochs. A Kolmogorov-Smirnov (KS) test was used to determine whether
280 the distributions of El Niño- and La Niña- associated local temperature and precipitation anomalies in
281 each region in 100-year Last Millennium epochs could statistically have been drawn from the same
282 population. There are detectable differences (at the 5% significance level) in the distribution of
283 ENSO-associated local climate variables in these 100-year epochs. West Pacific El Niño- and La
284 Niña- associated temperatures, for example, significantly vary in character through the Last
285 Millennium and with the historical 100-year epoch for the multi-model mean. Temporal changes in
286 local ENSO fingerprints ($\text{Corr}(\text{Local}, \text{Remote})$) of the Last Millennium, also likely result from external
287 forcings and/or internal ocean-atmosphere dynamics, which are discussed further in section 6.
288 However, these same relationships were not explored in the extended control simulations because of
289 the small number of contributions available from different models. Differing teleconnections may
290 result at different points in time and may also differ from present-day relationships. In addition, Last
291 Millennium variability in ENSO-local climate relationships across sites in the tropical Pacific
292 suggests that global ENSO changes do not necessarily scale linearly to local scales and cannot be
293 assumed to do so.

294 **5. ENSO under differing boundary conditions**

295 The CMIP5 archive also provides simulations of the mid-Holocene (midHolocene, circa 6,000 years
296 ago) from multiple participating climate models. The mid-Holocene provides a well-constrained
297 target for model-based studies (Schmidt et al., 2004) with substantially larger time-evolving forcings
298 than those imposed during the Last Millennium, and this period has also been the target of palaeo-
299 reconstructions. Hence, these simulations are also briefly investigated here, in addition to the
300 information provided by the Last Millennium experiment. Mid-Holocene simulations are run for at
301 least 100 years after reaching equilibrium and have changed orbital parameters and atmospheric
302 concentrations of greenhouse gases imposed. Other boundary conditions such as aerosols, solar
303 constant, vegetation and topography are prescribed as the same as in the pre-industrial control
304 simulation. We note that although the limited 100 model years contributed by various models may not
305 provide an exhaustive representation of ENSO behaviour in the mid-Holocene, they nonetheless
306 provide valuable insight into the potential influences of varying boundary conditions.

307 By way of context, Cobb et al. (2013) report that central Pacific corals record highly variable ENSO
308 activity through the Holocene, although no systematic trend in ENSO variance was demonstrated in
309 this study. A complementary Central Pacific reconstruction from Kiritimati Island suggests that
310 ENSO variance was persistently reduced by 79%, compared with today at this location about 4,300
311 years ago (McGregor et al., 2013). Central Pacific coral-based evidence of ENSO variability is
312 substantially different from lower-resolution records from the eastern equatorial Pacific (Conroy et
313 al., 2008; e.g. Moy et al., 2002). Collectively, East Pacific records suggest a systematic decrease in

314 mid-Holocene ENSO variance. On the West Pacific side of the basin, corals from northern Papua
315 New Guinea reveal a reduction in ENSO frequency and amplitude over the period of 7.6-5.4 ka
316 (thousand years ago) compared with today, and also identifies large and protracted El Niño events for
317 2.5–1.7 ka (McGregor and Gagan, 2004). These Mid-Holocene ENSO reconstructions do not
318 necessarily provide contradictory information, but may instead reflect geographic complexities (Carre
319 et al., 2014; Cobb et al., 2013). However, as proxy-based reconstructions from each of these regions
320 have been used to infer changes in the same coupled ocean-atmosphere system, we also examine
321 teleconnected ENSO patterns under these significantly different boundary conditions that characterise
322 the mid-Holocene.

323 In this study, we consider the subset of participating CMIP5 models with contributions of mid-
324 Holocene simulations (MRI-CGCM3, IPSL-CM5A-LR, FGOALS-s2, CCSM4) and find a general
325 reduction in spectral power across ENSO-relevant frequencies that has also been reported in model
326 experiments of this period conducted prior to the release of CMIP5 (Chiang et al., 2009). This
327 reduced spectral power in the ENSO band can be considered a metric for reduced ENSO amplitude
328 (Stevenson, 2012). Previous model and proxy-based studies have also hinted at subdued ENSO
329 activity in the mid-Holocene. For example, early studies using simple numerical models of the
330 coupled ocean-atmosphere system by Clement et al. (2000) demonstrate increasing ENSO variability
331 throughout the Holocene in response to time varying orbital forcings. The impact of mid-Holocene
332 orbital changes on ENSO variability has not been demonstrated comprehensively from proxy records.
333 However, various fossil coral reconstructions indicate that there may have been reductions in ENSO
334 variability in the mid-Holocene (Cobb et al., 2013).

335 In addition, when CMIP5 midHolocene model data are composited into positive (El Niño) and
336 negative (La Niña) phases, the magnitude of simulated mid-Holocene spatial patterns of ENSO
337 impacts (Supplementary Fig. 6) are subdued, relative to the historical. The relationship between
338 NINO3.4 mean surface temperature anomalies and regional (East, Central, West Pacific) temperature
339 and precipitation was also examined and shows particularly that the relationship between West Pacific
340 surface temperature anomalies and corresponding NINO3.4 temperature anomalies differs from the
341 midHolocene and historical simulations. The frequency of high and low local surface temperature
342 anomalies in the West Pacific during El Niño defined conditions is reduced in the midHolocene
343 experiment compared with the historical. The NINO3.4 impacts on East and Central Pacific regional
344 temperatures are broadly similar for the historical and mid-Holocene.

345 **6. Towards reconstructing robust ENSO histories**

346 This study uses palaeoclimate simulations conducted using a suite of CMIP5-participating models
347 with various forcing to investigate changes in ENSO and its teleconnections under differing boundary
348 conditions (the Last Millennium and mid-Holocene). The models show broadly similar global impacts

349 associated with NINO3.4 temperature anomalies between the Last Millennium and historical
350 experiments, although the magnitude of anomalies in the historical simulation is generally larger. We
351 find that ENSO-local climate relationships are typically weak in the West Pacific region, with remote-
352 local temperature relationships consistently stronger in the East and Central Pacific regions. The
353 relationships between NINO3.4 and local precipitation are weak and found to be significant only in
354 the Central Pacific. Furthermore, in the West Pacific particularly, El Niño- and La Niña- associated
355 temperatures vary significantly in character throughout the Last Millennium and with the historical
356 100-year epoch.

357 Previous studies of ENSO variability over the period encompassed in the CMIP5 past1000
358 simulations suggest that the most robust ENSO influence occurs over the Maritime Continent, in the
359 western part of the Pacific basin (Li et al., 2013). Overall, ENSO teleconnections over the pan-Pacific
360 region were found to be generally stronger when ENSO variance is higher. In our present study, we
361 find, conversely, that the correlation between West Pacific climates and NINO3.4 is lower than for the
362 Central and East Pacific, and also most variable between epochs. This apparent mismatch has several
363 possible causes. First, Li et al. (2013) focused on tree ring records, and the Maritime Continent region
364 they describe lies to the west of the West Pacific region we define to encompass published coral
365 records. This is likely an important difference in definition, due to the subtle shifts in the western
366 extent of the warm tongue characterising positive (El Niño) episodes, and conversely to the cool
367 anomalies characterising La Niña episodes. Furthermore, simulated climates of the Warm Pool region
368 are likely highly sensitive to model bias (Brown et al., 2012; 2013) and hence model dispersion is
369 expected (e.g., CCSM4 model in Fig. 7). Hence, subtle changes in the Pacific basin may impact this
370 region through several ocean-atmosphere mechanisms.

371 Although our current results appear to contradict those previously reported on ENSO teleconnections
372 (e.g., Li et al., 2013), collectively these studies suggest that remote reconstructions of ENSO require a
373 regional perspective. It may be inherently difficult to deconvolve variability in the NINO3.4 region
374 and local-scale, teleconnected climatic change in remote regions. Palaeoclimate studies often utilise
375 archives from single locations located in the Pacific Ocean to reconstruct generalised basin-scale
376 histories of ENSO. However, multiple studies demonstrate that proxies in one location alone should
377 not be considered regionally representative, or singularly insightful about robust ENSO
378 reconstructions without explicit examination of the stability of ENSO teleconnections. We argue that
379 proxy insights into change and variability in ENSO system are likely to be most robust when evidence
380 is synthesised over large spatial areas. That is, only incomplete information about temporal
381 changes in a large-scale climate system can be provided by considering changes at a singular location
382 (i.e. a time series of a climatic variable).

383 Considering multi-dimensional information in the form of spatial patterns of change through time is
384 likely to yield more robust insights in large-scale systems. This provides a framework for enhanced

385 interpretations of the invaluable information of palaeoclimatic change provided by proxy records. For
386 example, combined evidence from the West and Central Pacific is more likely to reveal the potentially
387 subtle changes in ENSO-associated spatial patterns of temperature and precipitation perturbations
388 across the Pacific. For remote regions outside the equatorial Pacific, the non-stationarity of ENSO
389 teleconnections is likely to be more problematic. These sites should be considered in conjunction with
390 palaeo-reconstructions from within the central Pacific basin, the so-called “centre of action” of ENSO
391 (Cobb et al., 2013). Under boundary conditions significantly different from present, such as the mid-
392 Holocene ENSO teleconnections are likely to be more variable, and hence potential non-stationarities
393 in local-remote relationships require explicit consideration in proxy interpretations. Spatially
394 integrated approaches have already been undertaken and provide valuable information over the recent
395 past (e.g. Li et al., 2013), and several multi-proxy reconstructions of ENSO are now available (e.g.,
396 Braganza et al., 2009; Wilson et al., 2010, Emile-Geay et al., 2013a; 2013b). Although these are often
397 limited in terms of temporal coverage to the past few centuries, or derived from extratropical record
398 and hence not directly representative of ENSO variability, they provide highly valuable records of
399 aspects of the ENSO system.

400 In this study, we investigated teleconnected changes using NINO3.4 to represent ENSO, which was
401 based on the determined similarity of the leading EOF of the multi-model mean in the historical and
402 Last Millennium simulations. However, important spatial changes in ENSO patterns are known to
403 occur and have been identified over the observational period (McPhaden et al., 2011), with impacts of
404 teleconnected patterns (Graf and Zanchettin, 2012). Furthermore, during periods of varying boundary
405 conditions, such as the mid-Holocene it is likely that while ENSO remained active, there was an
406 important change in the spatial pattern of the sea surface temperature anomalies (Karamperidou
407 and Di Nezio, 2015). This change in the spatial structure of ENSO was not explicitly explored here,
408 though explicit analysis of NINO3 and NINO4 (see Supplementary Fig. 1) may be insightful about
409 changes in the ENSO system and its teleconnections through time. In addition, various studies have
410 linked remote proxy variability to the tropical Pacific (e.g., Li et al., 2013) and hence it would be useful
411 in the future to investigate regions remote from the Pacific basin, such as in North America or China.
412 Regardless of the spatial dynamics of surface temperature anomalies in the NINO3.4 region, we do
413 not expect that the recommendation of considering proxy information from multiple is dependent on
414 the NINO3.4 metric used to define ENSO utilised here.

415 We have also identified decadal- to centennial-scale modulation of ENSO behaviour, which has been
416 highlighted previously (e.g., Karnauskas et al., 2012; Borlace et al., 2013). As such, a range of ENSO
417 variability may exist during the Last Millennium that is not fully revealed by the comparatively short
418 instrumental climate record. The existence of varying ENSO characteristics throughout the Last
419 Millennium is also supported by proxy-based climate reconstructions (Cobb et al., 2003), which show
420 variable ENSO characteristics include changing frequency and amplitude compared to modern during

421 the Last Millennium. In ENSO-sensitive regions, temporally limited proxy-based ENSO
422 reconstructions, such as from corals, may provide only a snapshot of ENSO history that cannot be
423 extrapolated through time. The decadal- to centennial-scale modulations of ENSO may plausibly
424 result from internal variability and/or external forcings, such as volcanic eruptions. We find multi-
425 decadal to centennial- scale El Niño- and La Niña-like phases in CMIP5 piControl simulations (with
426 no imposed external forcings). These are qualitatively similar to those shown in the externally forced
427 Last Millennium experiment, suggesting that multi-decadal ENSO modulation can be stochastic.
428 While Li et al. (2013), for example, agree that substantial stochastic ENSO modulation on these
429 timescales can occur, model-based studies indicate that CMIP5 simulations of the Last Millennium
430 demonstrate a more energetic and variable ENSO system on centennial timescales than in control runs
431 (Ault et al., 2013). In Ault et al.'s study, control simulations did not agree with a suite of recent
432 reconstructions while forced simulations are compatible, while Last Millennium simulations
433 demonstrate ENSO variability closer to reconstructions. Overall, Ault et al. (2013) suggest that ENSO
434 variability in models results from a thermodynamic response to reconstructed solar and volcanic
435 activity.

436 On seasonal to annual timescales, previous model evidence suggests the radiative forcing due to
437 volcanic stratospheric aerosols induces a La Niña episode that is followed by an El Niño episode after
438 the peak of the forcing (McGregor and Timmermann, 2011). The association of eruptions and
439 subsequent El Niño episodes has been demonstrated for forcings larger than that observed during the
440 historical period for Mt Pinatubo (Emile-Geay et al., 2008). For large volcanic eruptions, El Niño-like
441 conditions are favoured, with both the likelihood and amplitude of an El Niño episode subsequently
442 enhanced (Timmreck, 2012). Furthermore, proxy reconstructions derived from tree rings across the
443 Pacific reveal similar ENSO responses to those simulated, with anomalous cooling reconstructed in
444 the east-central tropical Pacific in the year of volcanic eruption, followed by anomalous warming
445 occurring one year after (Li et al., 2013). In this study, we also suggest that large tropical volcanic
446 eruptions occurring between 1250 and 1600 CE (Supplementary Fig. 7), may produce decadal- to
447 centennial-scale ENSO responses. We find, for example, that West Pacific El Niño- and La Niña-
448 associated temperatures differ in character through the Last Millennium and with the historical 100-
449 year epoch for the multi-model mean. The largest changes in this relationship occur in epochs
450 coinciding with the timing of major volcanic eruption (e.g., 1258, Samalas, 1458 Kuwae) (Fig. 7),
451 suggesting an extended influence of short-term volcanic forcings. Differences in ENSO-local climate
452 relationships in these epochs indicates a notable ENSO response to large volcanic eruptions and
453 suggests that short proxy records spanning periods of significant volcanic activity may be recording
454 temporally-specific influences.

455 Overall we suggest that 1) changes in ENSO do not necessarily scale linearly to local scale impacts,
456 2) that there is likely a sensitivity of ENSO to the background climate state and 3) the decadal- to

457 centennial-scale modulation of ENSO behaviour may arise from internal variability and/or external
458 forcings such as volcanic eruptions. However, we considered only a subset of CMIP5 models that
459 contributed palaeo-simulations and these contain systematic biases in ENSO representations (Power
460 et al., 2013). In their study focused on understanding ENSO responses to volcanic forcings, Emile-
461 Geay et al. (2008) suggested further forcing/response insights could be provided by GCMs with
462 realistic ENSO cycles and asked whether the current generation of models were up to the task.
463 Deficiencies in our theoretical knowledge of ENSO and the difficulties in representing physically
464 realistic ENSO cycles in GCMs (Guilyardi et al., 2012) are a limit on providing robust quantitative
465 understanding of forced and unforced changes in the ENSO system. Existing model simulations are
466 useful for examining palaeoclimates, despite their biases and reveal spatially and temporally complex
467 changes in ENSO and its teleconnected patterns under differing boundary conditions that should be
468 considered when developing robust proxy interpretations and ENSO histories in order that these are
469 most useful for constraining future ENSO behaviour under greenhouse forcings.

470 The palaeo-modelling type approaches utilised here do not attempt to replace proxy reconstructions,
471 but rather demonstrate that combining multiple approaches can provide enhanced interpretations of
472 reconstruction of past climate guiding our understanding of the most consistent physical explanations
473 for change (Schmidt, 2010). This study highlights several avenues for further model-based research
474 on ENSO variability and teleconnections:

- 475 • Several models have known difficulties simulating aspects of ENSO, such as the
476 nonlinear response of rainfall to extreme El Niño episodes (e.g., Cai et al., 2014). Additional
477 targeted experiments within a single climate model would provide further insight into the
478 apparent complexity of ENSO impacts through time.
- 479 • Our present study did not comprehensively investigate the relative influences on various
480 external forcings (solar and volcanics) and internal variability on ENSO characteristic, which
481 would provide useful information for comparison with proxy records. These mechanisms
482 could be investigated, for example, using a suite of simulations with single or varying
483 forcings, which may provide valuable general insight into ENSO response to external
484 forcings, including increased anthropogenic radiative forcings.
- 485 • More direct comparisons between model output and proxy reconstructions can be provided
486 by employing pseudo-proxy techniques. Using this approach, a simulated time series intended
487 to mimic actual proxy records ('pseudo-proxy') is generated from a climate model simulation
488 (Anchukaitis and Tierney, 2012). The pseudo-proxy approach can be used to interrogate the
489 necessary proxy density required for producing skilful regional climate field reconstructions
490 and provide guidance on interpretations of reconstructions from particular locations
491 (Smerdon, 2011; Wahl et al., 2014).

492

493 **Acknowledgements**

494 This research was supported by Australian Research Council Centre of Excellence for Climate
495 System Science (grant CE110001028). We thank NASA GISS for institutional support; resources
496 supporting this work were provided by the NASA High-End Computing (HEC) Program through the
497 NASA Center for Climate Simulation (NCCS) at Goddard Space Flight Center. We thank NOAA for
498 the C2D2 grant NA10OAR4310126 that supported the GISS-E2 last millennium simulations and
499 thank all the groups that contributed to the CMIP archive. We acknowledge the WCRP's Working
500 Group on Coupled Modelling, which is responsible for CMIP. The U.S. Department of Energy's
501 PCMDI provides CMIP5 coordinating support.

502

503 **Figure Captions**

504 **Figure Captions**

505 **Figure 1** Compositing anomaly maps for surface temperature (K) for CMIP5 models (left, El Niño
506 episodes; right, La Niña episodes) for historical experiment, showing multi-model mean (MMM) and
507 each model. Rectangular boxes indicate the West, Central and east Pacific regions.

508 **Figure 2** As for Figure 1, but showing composites from Last Millennium experiment.

509 **Figure 3** Comparison of leading patterns (standardised, first EOFs) of monthly variability in surface
510 temperature and precipitation for 20CR reanalysis (left: a, surface temperature; b, precipitation),
511 CMIP5 models (b, surface temperature; d, precipitation). CMIP5 historical patterns are the multi-
512 model mean (MMM) of the first EOF of each individual model for model years 1976-2005. Spatial
513 correlation coefficients between NINO3.4 index and 20CR precipitation (e) and the CMIP5 MMM
514 (f). Stippling indicates Spearman's rank correlations significant at the 95% level. Rectangular boxes
515 indicate the East, Central and West Pacific regions. Only model years 1976-2005 are used for
516 comparison as the historical experiment necessarily produces a non-stationary climate due to the time-
517 evolving anthropogenic greenhouse gas forcings imposed.

518 **Figure 4** Global mean NINO3.4 power spectrum (K^2 /unit frequency, black) of Last Millennium
519 simulations, relative to the red-noise (AR(1)) benchmark (dashed), for the multi-model mean (MMM)
520 and each model analysed. The historical simulation is shown in black and the 5th-95th percentile range
521 across the Last Millennium shown by purple envelope, calculated using 100-year epochs. Spectral
522 power was calculated using a Morlet wavelet of degree 6.

523 **Figure 5** Running annual-mean surface temperature anomalies (K) over the NINO3.4 region (5°N -
524 5°S, 170° - 120°W) for Last Millennium simulation for each model. Red/blue shading highlights
525 departures from each model's long-term mean. Running means were calculated using a 240-month
526 triangle smoother.

527 **Figure 6** Running annual-mean surface temperature anomalies (K) over the NINO3.4 region (5°N -
528 5°S, 170° - 120°W) for extended piControl simulations conducted with GISS-E2-R (a) and IPSL-
529 CM5A-LR (c) models. Red/blue shading highlights departures from each model's long-term mean.
530 Running means were calculated using a 240-month triangle smoother. Control simulations are spun
531 up to quasi-equilibrium and run for ideally >500 years, providing an arbitrary timeseries of model
532 internal variability. Global mean NINO3.4 power spectrum (K^2 /unit frequency, black), relative to the
533 red-noise (AR(1)) benchmark (dashed) for GISS-E2-R (b) and IPSL-CM5A-LR (d) models.

534 **Figure 7** Area-mean correlation coefficients (R) of NINO3.4 and local surface air temperature for the
535 East (black square), Central (red cross) and West (blue cross) for the MMM and each model. Data
536 points show correlation coefficients calculated for ten 100-year epochs comprising the Last

537 Millennium simulation and for the historical simulation (1906-2005). Plot markers in grey indicate
538 correlations that are not statistically significant (at the 5% significance level).

539 **Figure 8** As for Figure 7 but showing correlation coefficients (R) of NINO3.4 and local precipitation.

540 **Table Caption**

541 **Table 1.** Details of CMIP5 experiments and models analysed. Further details can be found through
542 the Program for Climate Model Diagnosis and Intercomparison (PCMDI).

543

544

545 **Supplementary Figure Captions**

546 **Supplementary Figure 1** Location of NINO3, NINO3.4 and NINO4 index regions.

547 **Supplementary Figure 2** Composit ed anomaly maps for surface temperature (K) for CMIP5 models
548 for El Niño episodes for historical experiment (left) and past1000 experiment (right), showing multi-
549 model mean (MMM). El Niño events are defined using the NINO3.4 (upper), NINO3 (middle) and
550 NINO4 (lower) indices. Rectangular boxes indicate the West, Central and east Pacific regions. Plots
551 indicate that teleconnected patterns may differ with ENSO index considered.

552 **Supplementary Figure 3** As for Supplementary Figure 2 but showing composit ed La Niña episodes.

553 **Supplementary Figure 4** Running annual-mean surface temperature anomalies (K) over the
554 NINO3.4 region (5°N - 5°S, 170° - 120°W) for Last Millennium simulations conducted with MIROC-
555 ESM and bcc-csm1-1 models. Red/blue shading highlights departures from each model's long-term
556 mean. Running means were calculated using a 240-month triangle smoother.

557 **Supplementary Figure 5** Comparison of leading patterns (standardised, first EOFs) of monthly
558 variability in surface temperature for CMIP5 multi-model mean (MMM) for (a) historical and (b) Last
559 Millennium experiments. The location of the NINO3.4 region (5°N - 5°S, 170° - 120°W) is indicated
560 by a rectangular box.

561 **Supplementary Figure 6** Composit ed anomaly maps for surface temperature (K) for CMIP5 models
562 (left, El Niño episodes; right, La Niña episodes) for midHolocene experiment, showing multi-model
563 mean (MMM) and each model. Rectangular boxes indicate the West, Central and east Pacific regions.

564 **Supplementary Figure 7** Evolution of prescribed volcanic forcings for CMIP5 Last Millennium
565 experiment, showing the two alternative data sets used by modelling groups, including (a) timeseries
566 of stratospheric aerosol optical depth (AOD) at 0.55µm provided by Crowley et al. (2008) and (b)
567 global hemisphere total stratospheric injections (Tg) from Gao et al. (2008). Large volcanic eruptions
568 occurring between 1200 and 1500 are evident in both data sets.

569

570

571 **References**

- 572 Anchukaitis, K. J. and Tierney, J. E.: Identifying coherent spatiotemporal modes in time-uncertain
573 proxy paleoclimate records, *Climate Dynamics*, doi:10.1007/s00382-012-1483-0, 2012.
- 574 Ault, T. R., Deser, C., Newman, M. and Emile-Geay, J.: Characterizing decadal to centennial
575 variability in the equatorial Pacific during the last millennium, *Geophysical Research Letters*, 40(13),
576 3450–3456, doi:10.1002/grl.50647, 2013.
- 577 Bellenger, H., Guilyardi, E. , Leloup, J., Lengaigne, M. and Vialard, J.: ENSO representation in
578 climate models: from CMIP3 to CMIP5, *Climate Dynamics*, 42(7-8), 1999–2018,
579 doi:10.1007/s00382-013-1783-z, 2013.
- 580 Borlace, S., Cai, W. and Santoso, A.: Multidecadal ENSO Amplitude Variability in a 1000-yr
581 Simulation of a Coupled Global Climate Model: Implications for Observed ENSO Variability, *Journal*
582 *of Climate*, 26(23), 9399–9407, doi:10.1175/JCLI-D-13-00281.1, 2013.
- 583 Braganza, K., Gergis, J. L., Power, S. B., Risbey, J. S. and Fowler, A. M.: A multiproxy index of the
584 El Niño–Southern Oscillation, A.D. 1525–1982, *Journal of Geophysical Research Atmospheres*,
585 114(D5), D05106, doi:10.1029/2008JD010896, 2009.
- 586 Brown, J. N., Gupta, Sen, A., Brown, J. R., Muir, L. C., Risbey, J. S., Whetton, P., Zhang, X.,
587 Ganachaud, A., Murphy, B. and Wijffels, S. E.: Implications of CMIP3 model biases and
588 uncertainties for climate projections in the western tropical Pacific, *Climatic Change*, 119(1), 147–
589 161, doi:10.1007/s10584-012-0603-5, 2012.
- 590 Brown, J. N., Langlais, C. and Maes, C.: Zonal structure and variability of the Western Pacific
591 dynamic warm pool edge in CMIP5, *Climate Dynamics*, 42(11-12), 3061–3076, doi:10.1007/s00382-
592 013-1931-5, 2013.
- 593 Cai, W., Borlace, S., Lengaigne, M. and Van Rensch, P.: Increasing frequency of extreme El Niño
594 events due to greenhouse warming, *Nature Climate Change* doi:10.1038/nclimate2100, 2014.
- 595 Carre, M., Sachs, J. P., Purca, S., Schauer, A. J., Braconnot, P., Falcon, R. A., Julien, M. and
596 Lavallee, D.: Holocene history of ENSO variance and asymmetry in the eastern tropical Pacific,
597 *Science*, doi:10.1126/science.1252220, 2014.
- 598 Chiang, J. C. H., Fang, Y. and Chang, P.: Pacific Climate Change and ENSO Activity in the Mid-
599 Holocene, *Journal of Climate*, 22(4), 923–939, doi:10.1175/2008JCLI2644.1, 2009.
- 600 Clement, A. C., Seager, R. and Cane, M. A.: Suppression of El Niño during the Mid-Holocene by
601 changes in the Earth's orbit, *Paleoceanography*, 15(6), 731–737, 2000.
- 602 Coats, S., Smerdon, J. E. and Cook, B. I.: Stationarity of the tropical pacific teleconnection to North

603 America in CMIP5/PMIP3 model simulations, *Geophysical Research Letters*, 40, 4927–4932,
604 doi:10.1002/grl.50938, 2013.

605 Cobb, K. M., Charles, C. D., Cheng, H. and Edwards, R. L.: El Niño/Southern Oscillation and tropical
606 Pacific climate during the last millennium, *Nature*, 424(6946), 271–276, doi:10.1038/nature01779,
607 2003.

608 Cobb, K. M., Westphal, N., Sayani, H. R., Watson, J. T., Di Lorenzo, E., Cheng, H., Edwards, R. L.
609 and Charles, C. D.: Highly Variable El Niño-Southern Oscillation Throughout the Holocene, *Science*,
610 339(6115), 67–70, doi:10.1126/science.1228246, 2013.

611 Collins, M., An, S.-I., Cai, W., Ganachaud, A., Guilyardi, E., Jin, F.-F., Jochum, M., Lengaigne, M.,
612 Power, S., Timmermann, A., Vecchi, G. and Wittenberg, A.: The impact of global warming on the
613 tropical Pacific Ocean and El Niño, *Nature Geoscience*, 3(6), 391–397, doi:10.1038/ngeo868, 2010.

614 Compo, G. P. and Whitaker, J. S.: The Twentieth Century Reanalysis Project, *Quarterly Journal of the*
615 *Royal Meteorological Society*, 2011.

616 Conroy, J. L., Overpeck, J. T., Cole, J. E., Shanahan, T. M. and Steinitz-Kannan, M.: Holocene
617 changes in eastern tropical Pacific climate inferred from a Galápagos lake sediment record,
618 *Quaternary Science Reviews*, 27(11-12), 1166–1180, doi:10.1016/j.quascirev.2008.02.015, 2008.

619 Crowley, T. J., Zielinski, G., Vinther, B., Udisti, R., Kreutz, K., Cole-Dai, J. and Castellano, J.:
620 Volcanism and the Little Ice Age, *PAGES Newsletter*, 16, 22–23, doi:10.1029/2002GL0166335,
621 2008.

622 DiNezio, P. N., Kirtman, B. P., Clement, A. C., Lee, S.-K., Vecchi, G. A. and Wittenberg, A.: Mean
623 Climate Controls on the Simulated Response of ENSO to Increasing Greenhouse Gases, *Journal of*
624 *Climate*, 25(21), 7399–7420, doi:10.1175/JCLI-D-11-00494.1, 2012.

625 Emile-Geay, J., Seager, R., Cane, M. A., Cook, E. R. and Haug, G. H.: Volcanoes and ENSO over the
626 Past Millennium, *Journal of Climate*, 21(13), 3134–3148, doi:10.1175/2007JCLI1884.1, 2008.

627 Emile-Geay, J., Cobb, K. M., Mann, M. E. and Wittenberg, A. T.: Estimating Central Equatorial
628 Pacific SST Variability over the Past Millennium. Part I: Methodology and Validation, *Journal of*
629 *Climate*, 26(7), 2302–2328, doi:10.1175/JCLI-D-11-00510.1, 2013a.

630 Emile-Geay, J., Cobb, K. M., Mann, M. E. and Wittenberg, A. T.: Estimating Central Equatorial
631 Pacific SST Variability over the Past Millennium. Part II: Reconstructions and Implications, *Journal*
632 *of Climate*, 26(7), 2329–2352, doi:10.1175/JCLI-D-11-00511.1, 2013b.

633 England, M. H., McGregor, S., Spence, P., Meehl, G. A., Timmermann, A., Cai, W., Gupta, A. S.,
634 McPhaden, M. J., Purich, A. and Santoso, A.: Recent intensification of wind-driven circulation in the
635 Pacific and the ongoing warming hiatus, *Nature*, 4(3), 222–227, doi:10.1038/nclimate2106, 2014.

636 Gallant, A. J. E., Phipps, S. J., Karoly, D. J., Mullan, A. B. and Lorrey, A. M.: Nonstationary
637 Australasian Teleconnections and Implications for Paleoclimate Reconstructions, *Journal of Climate*,
638 26(22), 8827–8849, doi:10.1175/JCLI-D-12-00338.1, 2013.

639 Gao, C., Robock, A. and Ammann, C.: Volcanic forcing of climate over the past 1500 years: An
640 improved ice core-based index for climate models, *Journal of Geophysical Research Atmospheres*,
641 113(D23), D23111, doi:10.1029/2008JD010239, 2008.

642 Guilyardi, E., Bellenger, H., Collins, M., Ferrett, S., Cai, W. and Wittenberg, A.: A first look at
643 ENSO in CMIP5, *Clivar Exchanges*, 17(1), 29–32, 2012.

644 Graf, H.-F. and Zanchettin, D.: Central Pacific El Niño, the “subtropical bridge,” and Eurasian
645 climate, *Journal of Geophysical Research Atmospheres*, 117(D1), D01102,
646 doi:10.1029/2011JD016493, 2012.

647 Gupta, A. S., Jourdain, N. C., Brown, J. N. and Monselesan, D.: Climate Drift in the CMIP5 Models*,
648 *Journal of Climate*, 26(21), 8597–8615, doi:10.1175/JCLI-D-12-00521.s1, 2013.

649 Karamperidou, C. and Di Nezio, P. N.: The response of ENSO flavors to mid-Holocene climate:
650 Implications for proxy interpretation, *Paleoceanography*, doi:10.1002/2014PA002742, 2015.

651 Karaukas, K. B., Smerdon, J. E., Seager, R. and González-Rouco, J. F.: A Pacific Centennial
652 Oscillation Predicted by Coupled GCMs*, *Journal of Climate*, 25(17), 5943–5961, doi:10.1175/JCLI-
653 D-11-00421.1, 2012.

654 Khider, D., Stott, L. D., Emile-Geay, J., Thunell, R. and Hammond, D. E.: Assessing El Niño
655 Southern Oscillation variability during the past millennium, *Paleoceanography*, 26(3),
656 doi:10.1029/2011PA002139, 2011.

657 King, A. D., Donat, M. G., Alexander, L. V. and Karoly, D. J.: The ENSO-Australian rainfall
658 teleconnection in reanalysis and CMIP5, *Climate Dynamics*, doi:10.1007/s00382-014-2159-8, 2014.

659 Klingaman, N. P. and Woolnough, S. J.: On the drivers of inter-annual and decadal rainfall variability
660 in Queensland, Australia, *International Journal of Climatology*, 33, 2413–2430, doi: 0.1002/joc.3593,
661 2013.

662 Lewis, S. C., LeGrande, A. N., Schmidt, G. A. and Kelley, M.: Comparison of forced ENSO-like
663 hydrological expressions in simulations of the pre-industrial and mid-Holocene, *Journal of*
664 *Geophysical Research Atmospheres*, doi:10.1002/(ISSN)2169-8996, 2014.

665 Li, J., Xie, S.-P., Cook, E. R., Huang, G., D'Arrigo, R., Liu, F., Ma, J. and Zheng, X.-T.: Interdecadal
666 modulation of El Niño amplitude during the past millennium, *Nature Climate Change*, 1(2), 114–118,
667 doi:10.1038/nclimate1086, 2011.

668 Li, J., Xie, S.-P., Cook, E. R., Morales, M. S., Christie, D. A., Johnson, N. C., Chen, F., D'Arrigo, R.,
669 Fowler, A. M., Gou, X. and Fang, K.: El Niño modulations over the past seven centuries, *Nature*
670 *Climate Change*, 3(9), 822–826, doi:10.1038/nclimate1936, 2013.

671 Lorenz, R., Davin, E. L. and Seneviratne, S. I.: Modeling land-climate coupling in Europe: Impact of
672 land surface representation on climate variability and extremes, *Journal of Geophysical Research:*
673 *Atmospheres* (1984–2012), 117(D20), 2012.

674 McGregor, H. V. and Gagan, M. K.: Western Pacific coral $\delta^{18}\text{O}$ records of anomalous Holocene
675 variability in the El Niño–Southern Oscillation, *Geophysical Research Letters*, 31(11),
676 doi:10.1029/2004GL019972, 2004.

677 McGregor, H. V., Fischer, M. J., Gagan, M. K., Fink, D., Phipps, S. J., Wong, H. and Woodroffe, C.
678 D.: A weak El Niño/Southern Oscillation with delayed seasonal growth around 4,300 years ago,
679 *Nature Geoscience*, 6(11), 949–953, doi:10.1038/ngeo1936, 2013.

680 McGregor, S. and Timmermann, A.: The Effect of Explosive Tropical Volcanism on ENSO, *Journal*
681 *of Climate*, 24(8), 2178–2191, doi:10.1175/2010JCLI3990.1, 2011.

682 McPhaden, M. J., Lee, T. and McClurg, D.: El Niño and its relationship to changing background
683 conditions in the tropical Pacific Ocean, *Geophysical Research Letters*, 38(15),
684 doi:10.1029/2011GL048275, 2011.

685 Moy, C., Seltzer, G., Rodbell, D. and Anderson, D.: Variability of El Niño/Southern Oscillation
686 activity at millennial timescales during the Holocene epoch, *Nature*, 420, 162–165,
687 doi:10.1038/nature01194, 2002.

688

689 Pascolini-Campbell, M., Zanchettin, D., Bothe, O., Timmreck, C., Matei, D., Jungclaus, J. H. and
690 Graf, H. F.: Toward a record of Central Pacific El Niño events since 1880, *Theoretical and Applied*
691 *Climatology*, 119(1-2), 379–389, doi:10.1007/s00704-014-1114-2, 2014.

692 Power, S., Delage, F., Chung, C., Kociuba, G. and Keay, K.: Robust twenty-first-century projections
693 of El Niño and related precipitation variability, *Nature*, 502(7472), 541–545,
694 doi:10.1038/nature12580, 2013.

695 Schmidt, G. A.: Enhancing the relevance of palaeoclimate model/data comparisons for assessments of
696 future climate change, edited by C. Caseldine, C. Turney, and A. Long, *Journal of Quaternary*
697 *Science*, 25(1), 79–87, doi:10.1002/jqs.1314, 2010.

698 Schmidt, G. A., Kelley, M., Nazarenko, L., Ruedy, R., Russell, G. L., Aleinov, I., Bauer, M., Bauer,
699 S. E., Bhat, M. K., Bleck, R., Canuto, V., Chen, Y.-H., Cheng, Y., Clune, T. L., Del Genio, A., de
700 Fainchtein, R., Faluvegi, G., Hansen, J. E., Healy, R. J., Kiang, N. Y., Koch, D., Lacis, A. A.,

701 LeGrande, A. N., Lerner, J., Lo, K. K., Matthews, E. E., Menon, S., Miller, R. L., Oinas, V., Oloso,
702 A. O., Perlwitz, J. P., Puma, M. J., Putman, W. M., Rind, D., Romanou, A., Sato, M., Shindell, D. T.,
703 Sun, S., Syed, R. A., Tausnev, N., Tsigaridis, K., Unger, N., Voulgarakis, A., Yao, M.-S. and Zhang,
704 J.: Configuration and assessment of the GISS ModelE2 contributions to the CMIP5 archive, *Journal*
705 *of Advance in Modeling Earth Systems*, 6(1), 141–184, doi:10.1002/2013MS000265, 2014.

706 Schmidt, G. A., Shindell, D. T., Miller, R. L., Mann, M. E. and Rind, D.: General circulation
707 modelling of Holocene climate variability, *Quaternary Science Reviews*, 23(20-22), 2167–2181,
708 doi:10.1016/j.quascirev.2004.08.005, 2004.

709 Smerdon, J. E.: Climate models as a test bed for climate reconstruction methods: pseudoproxy
710 experiments, *WIREs Clim Change*, 3(1), 63–77, doi:10.1002/wcc.149, 2011.

711 Stevenson, S. L.: Significant changes to ENSO strength and impacts in the twenty-first century:
712 Results from CMIP5, *Geophysical Research Letters*, 39(17), L17703, doi:10.1029/2012GL052759,
713 2012.

714 Taylor, K. E., Stouffer, R. J. and Meehl, G. A.: An overview of CMIP5 and the experiment design,
715 *Bulletin of the American Meteorological Society*, 93(4), 485, doi:10.1175/BAMS-D-11-00094.1,
716 2012.

717 Timmreck, C.: Modeling the climatic effects of large explosive volcanic eruptions, *WIREs Clim*
718 *Change*, 3(6), 545–564, doi:10.1002/wcc.192, 2012.

719 Torrence, C. and Compo, G. P.: A practical guide to wavelet analysis, *Bulletin of the American*
720 *Meteorological Society*, 79(1), 61–78, 1998.

721 Trenberth, K. E.: The Definition of El Nino, *Bulletin of the American Meteorological Society*, 78(12),
722 2771–2777, 1997.

723 Vecchi, G. A. and Wittenberg, A. T.: El Niño and our future climate: where do we stand? *WIREs*
724 *Climate Change*, 1(2), 260–270, 2010.

725 Wahl, E. R., Diaz, H. F., Smerdon, J. E. and Ammann, C. M.: Global and Planetary Change, *Global*
726 *and Planetary Change*, 122(C), 1–13, doi:10.1016/j.gloplacha.2014.08.005, 2014.

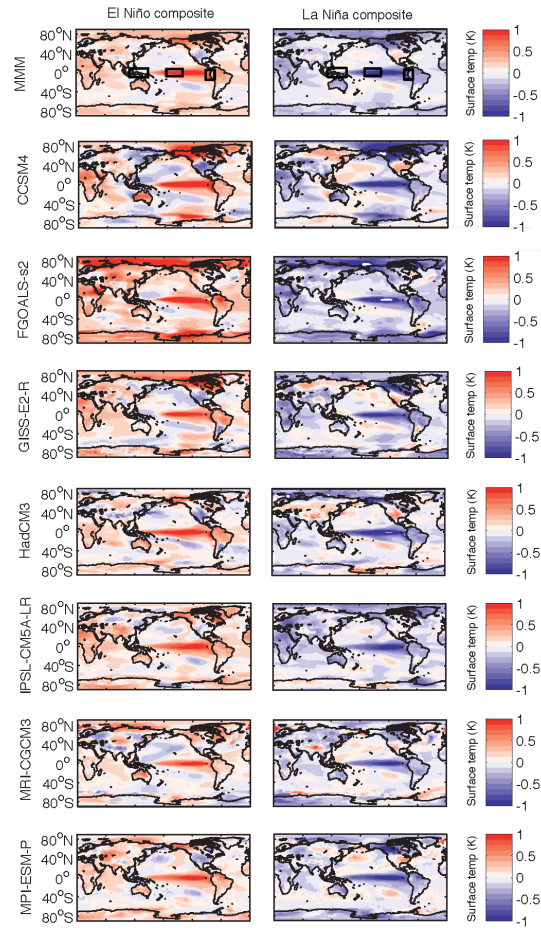
727 Wilson, R., Cook, E., D'Arrigo, R., Riedwyl, N., Evans, M. N., Tudhope, A. and Allan, R.:
728 Reconstructing ENSO: the influence of method, proxy data, climate forcing and teleconnections,
729 edited by C. Caseldine, C. Turney, and A. Long, *Journal of Quaternary Science*, 25(1), 62–78,
730 doi:10.1002/jqs.1297, 2010.

731 Wittenberg, A. T.: Are historical records sufficient to constrain ENSO simulations? *Geophysical*
732 *Research Letters*, 36(12), 2009.

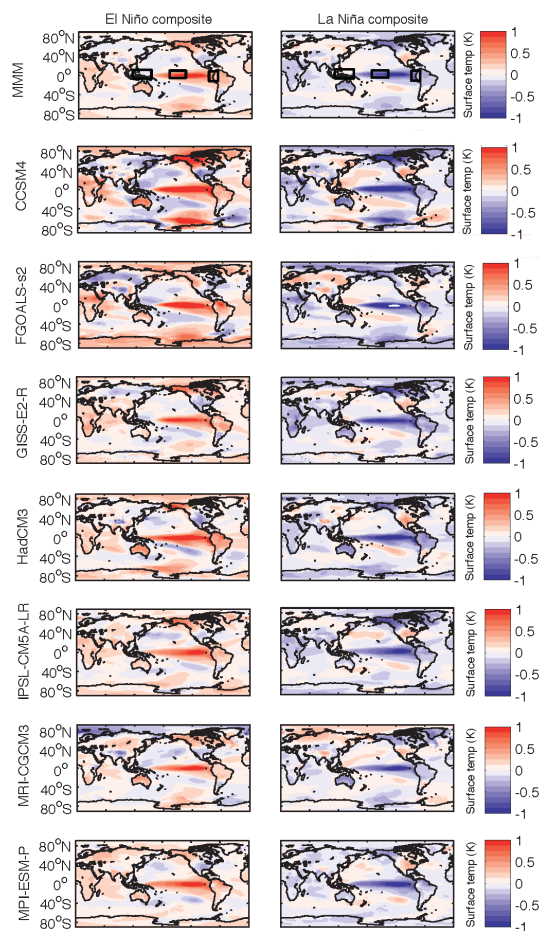
733

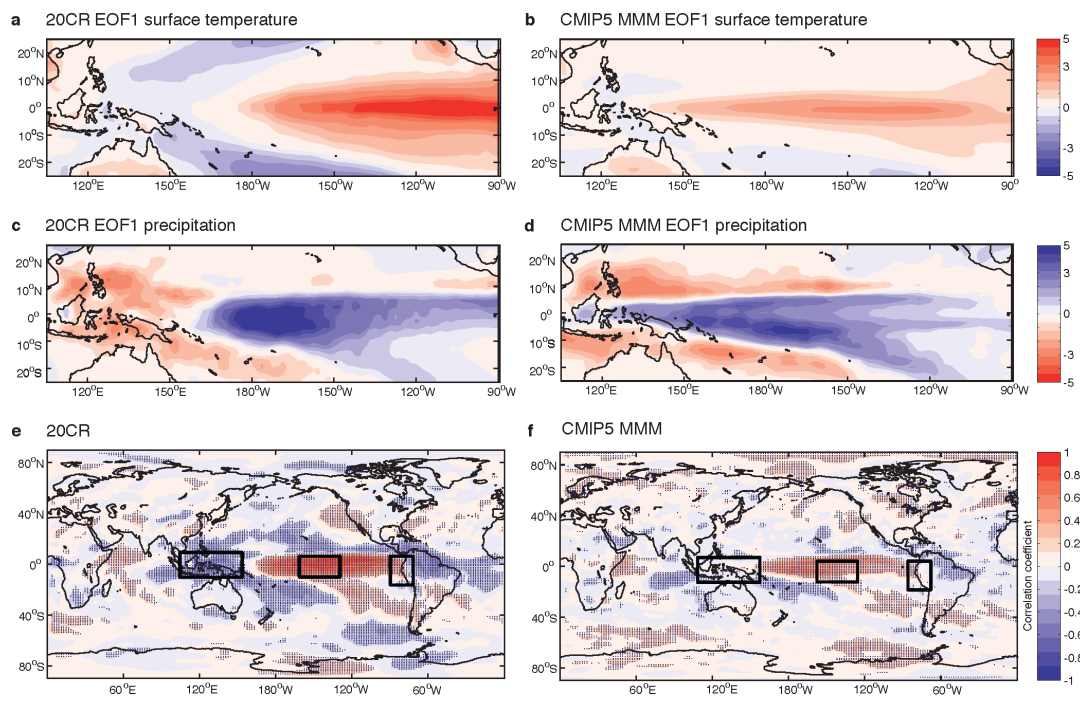
735 Figures

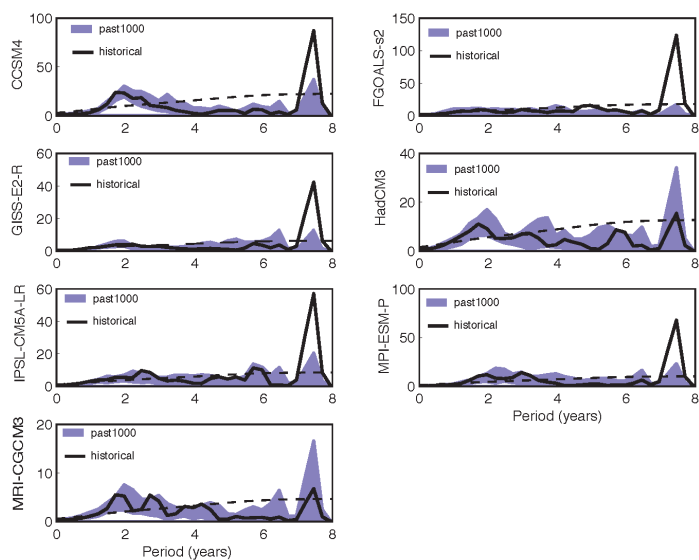
736 Figure 1

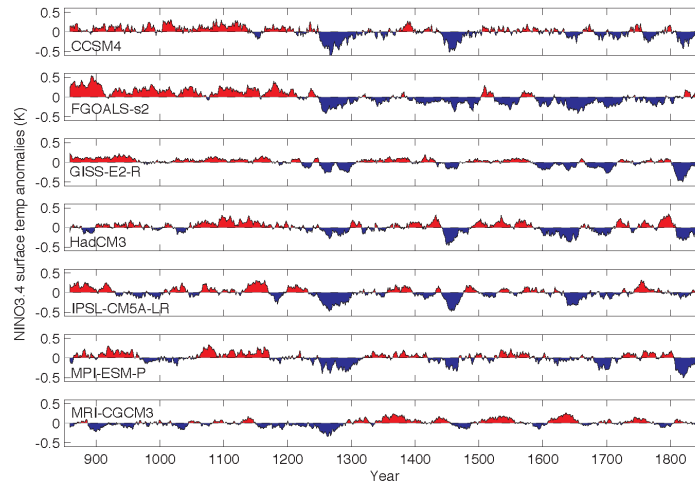


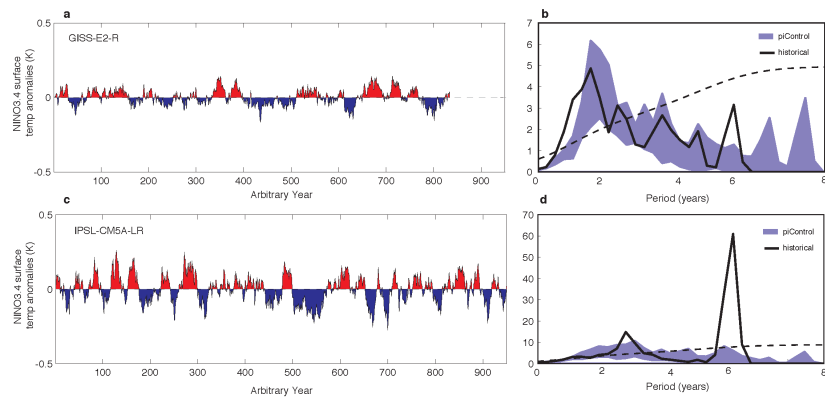
737

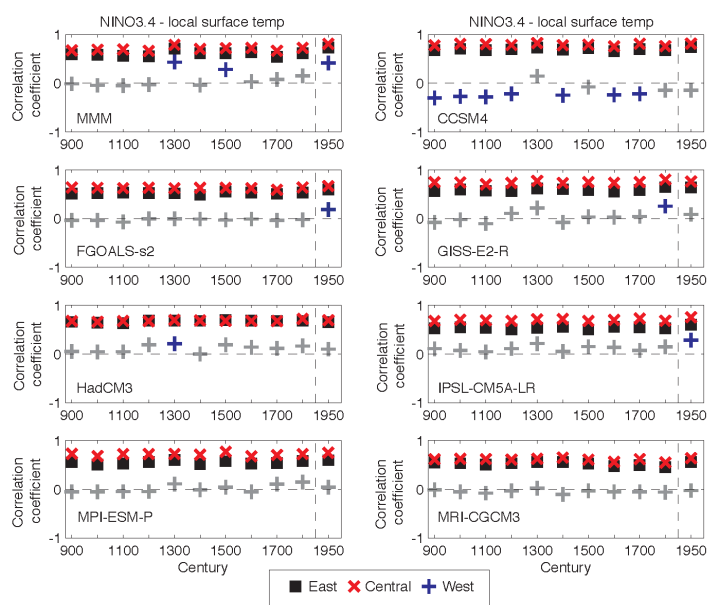


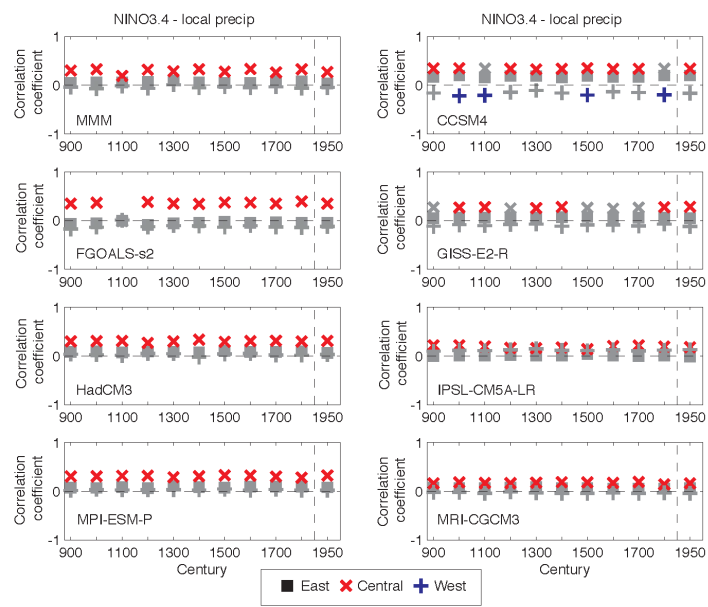












752 **Table 1.** Details of CMIP5 experiments and models analysed. Further details can be found through
 753 the Program for Climate Model Diagnosis and Intercomparison (PCMDI).

Experiment	Major forcings	Years Analysed	Models
historical	Time-evolving anthropogenic (greenhouse gases, aerosols, ozone) and natural (solar, volcanics)	1906-2005 CE	CCSM4, FGOALS-s2, GISS-E2-R, HadCM3, IPSL-CM5A-LR, MPI-ESM-P, MRI-CGCM3
past1000	Time-evolving greenhouse gases, solar, volcanics, land use and orbital parameters	850-1849 CE	CCSM4, FGOALS-s2, GISS-E2-R, HadCM3, IPSL-CM5A-LR, MPI-ESM-P, MRI-CGCM3
piControl	Non-evolving pre-industrial forcings	All	GISS-E2-R, IPSL-CM5A-LR

754

755